Microcrystallography With *In Meso* Grown Membrane Protein Crystals

Vadim Cherezov, Michael Hanson, Peter Kuhn and Raymond C. Stevens

Department of Molecular Biology, The Scripps Research Institute, La Jolla, CA

This work was supported by NIH Roadmap grant P50 GM073197.

Abstract

Membrane protein crystallization in lipidic cubic phases (or *in meso*) often produces small but very well ordered crystals. They appear to be a perfect match for the recently commissioned minibeam capability at the GM/CA CAT at Advanced Photon Source, Argonne, IL. We describe challenges and solutions to the problems related to growing, manipulating and collecting data of *in meso* grown microcrystals. Primary attention is focused on automated setting up nanoliter-scale lipidic cubic phase (LCP) crystallization drops, visual detection of initial crystals hits of colorless proteins in LCP, harvesting microcrystals from LCP, alignment of invisible microcrystal embedded in opaque frozen lipidic mesophase with 10 μm in diameter minibeam, and strategies for data collection. Using technologies developed under this project we recently determined a structure of a modified β2-adrenergic receptor at 2.4 Å resolution (Cherezov et al., 2007; Rosenbaum et al., 2007). Directions for extending utility of microcrystallography with frozen as well as *in situ* crystals are proposed.

In meso crystallization.

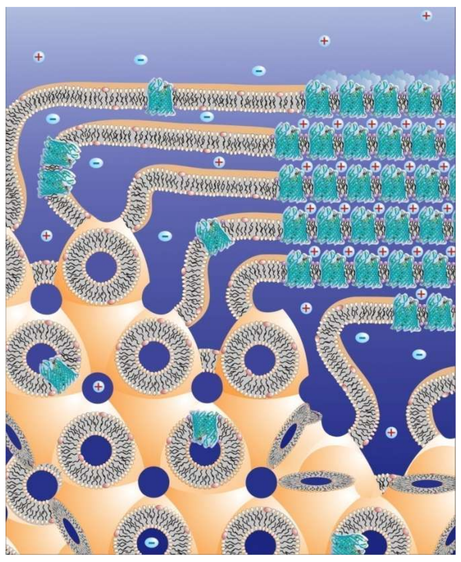

Cartoon representation of a membrane protein crystal growing in lipidic mesophase.

- Proteins are embedded in lipid bilayer
- Proteins diffuse in 3-D
- Multilamellar lipid portal surrounds growing crystal

Robotics for *in meso* crystallization.

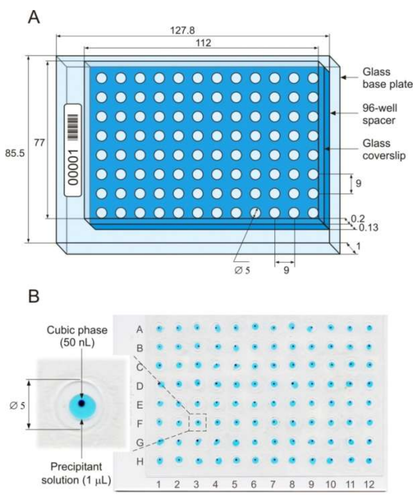

Glass sandwich plates with excellent optical properties (Cherezov et al, 2004).

- Standard SBS footprint
- Low-profile (< 2 mm)
- Non-birefringent
- Lipidic mesophase is sandwiched between two flat glass sheets
- Extremely low dehydration rate (crystals remain intact for over 1 year)
- Well can be individually opened for crystal harvesting
- Possible to use plastic sheets instead of glass for *in situ* diffraction

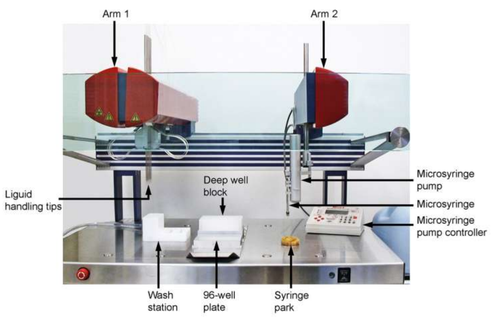

In meso crystallization robot (Cherezov et al, 2004)

- Less than 10 min setup for 96-well plate
- Typical LCP dispensing volume: 20 – 50 nL
- Minimum LCP dispensing volume: 0.5 nL
- Typical precipitant volume: 0.8 μL

RockImager 1000 (Formulatrix, Inc). Automatic incubator/imager.

- Handles most crystallization plates with SBS footpring including glass sandwich plates
- Incubator for 1000 plates
- 12x zoom lens
- Polarizers
- Variable condenser
- Versatile drop finding algorithms
- Comprehensive database

Crystal detection *in meso*.

Automatic lipid phase finding algorithm: detects precipitant drop, finds lipidic mesophase drop and optically zooms into it.

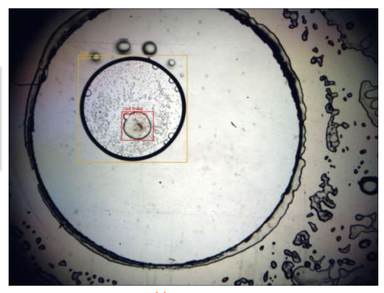

Zoomed in images are taken at several depth levels and combined together to produce a combine extended focus image.

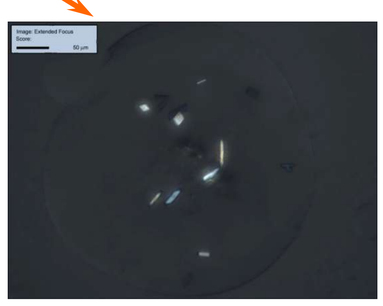

In addition to normal light images, cross-polarized images allow to confirm crystallinity and detect crystals hidden in precipitate or lipid mesophase defects.

Detection of micron-size crystals

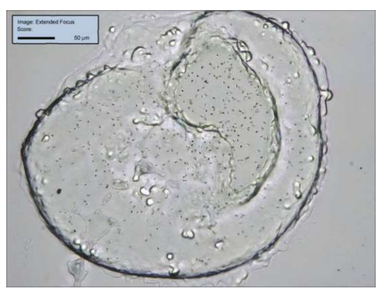

Even very small (<5 μm) crystals can be visually detected in most cases. Showers of small microcrystals are typical for initial hits.

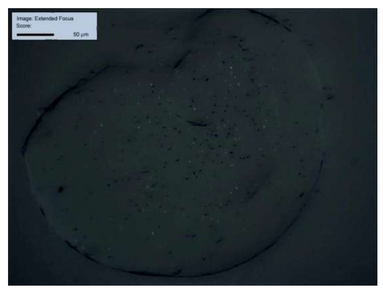

Cross-polarized images help to confirm that the objects of interest are crystalline and not just droplets or other defects in lipidic mesophase.

Minibeam at 23-ID beamline GM/CA CAT, APS, Argonne

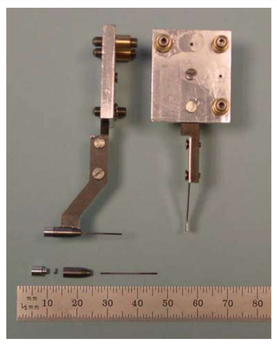

Microcollimator can hold 5 or 10 μm aperture. Kinematic mount allows for rapid interchangeability between collimators

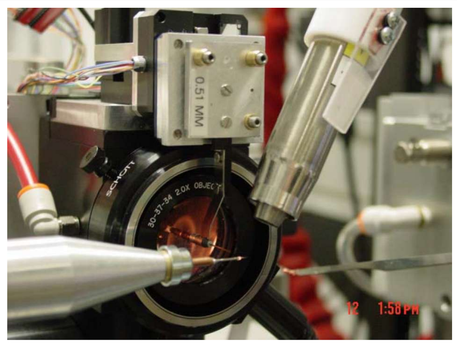

Minibeam setup at 23-ID beamline featuring microcollimator , inline optics, crystal mount attached to a goniometer head, cryo-stream and a beamstop

Microcrystal alignment

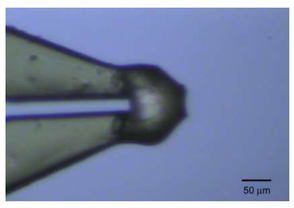

Microcrystals embedded in opaque frozen lipidic mesophase are invisible. Crystal alignment is performed by diffraction.

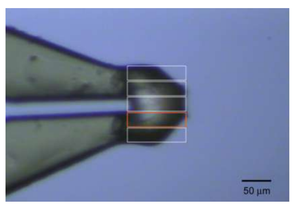

Step 1. Coarse scanning with 100 x 25 μm slitted beam using 30 μm steps

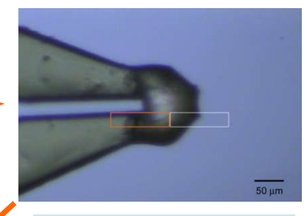

Step 2. Confinement of the crystal location into an area of 50 x 25 μm

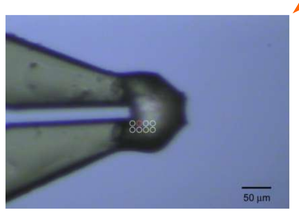

Step 3. Coarse scanning with 10 μm minibeam using 15 μm step

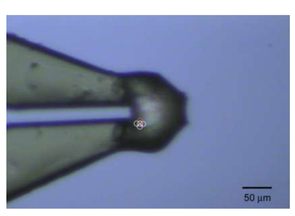

Step 4. Fine-tuning the crystal position with 10 μm minibeam using 3-5 μm steps.

Step 5. Rotate the loop 90° and repeat alignment with 10 μm minibeam in vertical direction only using coarse 15 μm and fine 3 μm steps.

Caution: even after alignment small microcrystals drift out of the minibeam during data collection and have to be readjusted after each 10-20° of rotation.

Microdiffraction

Diffraction resolution from *in meso* grown crystals scales roughly with crystal size

Crystals of b2AR-T4L with average size 30 x 15 x 5 μm

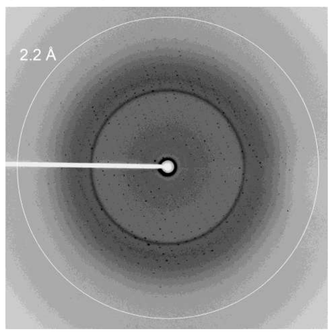

Diffract to 2.2 Å resolution using 10 μm minibeam.
Caution: minibeam intensity should be fairly high to capture weak high-resolution spots, leading to inevitable crystal damage.

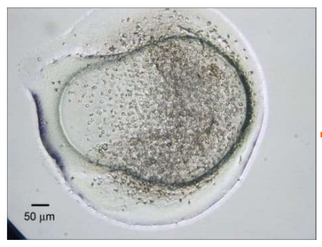

Very small microcrystals of Band 3 with typical size 8 x 8 x 4 μm

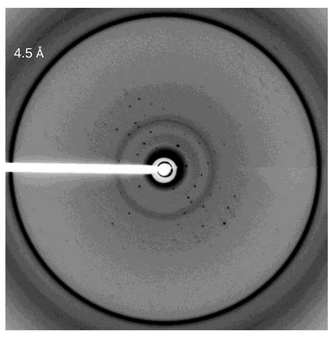

Produce useful diffraction to ~7 Å resolution using 10 μm minibeam

Minibeam significantly increases signal/noise ratio and resolution limit for microcrystals

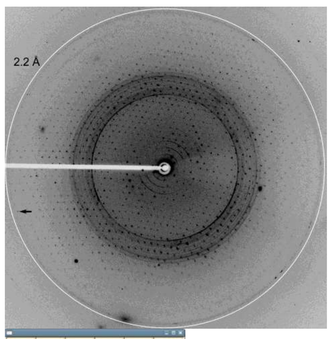

10 μm minibeam
2.3 Å spot
S/N ~ 118/32 = 3.7

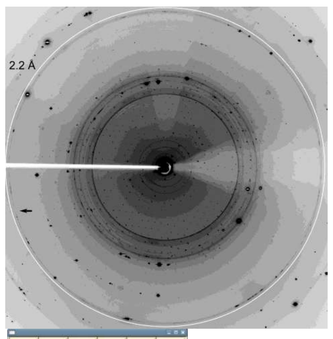

150 x 75 μm beam
2.3 Å spot
S/N ~ 2900/2100 = 1.4

Bacteriorhodopsin crystal (30 x 30 x 5 μm) is exposed at the same position and orientation using either 10 μm minibeam or slitted 150 x 75 μm beam with the same attenuation and exposure time. The same diffraction spot pointed by an arrow is enlarged to demonstrate increase in signal/noise ratio.

Radiation damage is an inherent challenge of microcrystallography

Small microcrystals survive for only few exposures under intense minibeam

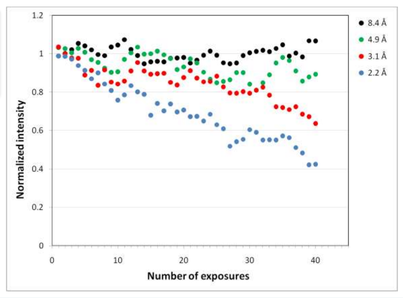

Bacteriorhodopsin crystal (30 x 30 x 5 μm) is repeatedly exposed 40 times at the same position and orientation using 10 μm minibeam. Changes in intensity of 4 spots at different resolution with number of exposures are shown in the figure.

References

Cherezov, V., Rosenbaum, D.M., Hanson, M.A., Rasmussen, S.G.F., Thian, F.S., Kobilka, T.S., Choi, H.-J., Kuhn, P., Weis, W.I., Kobilka, B.K., Stevens, R.C. High resolution crystal structure of an engineered human β2-adrenergic G protein-coupled receptor. *Science*, 25 October 2007 (10.1126/science.1150577)

Rosenbaum, D.M., Cherezov, V., Hanson, M.A., Rasmussen, S.G.F., Thian, F.S., Kobilka, T.S., Choi, H.-J., Yao, X.-J., Weis, W.I., Stevens, R.C, Kobilka, B.K. GPCR engineering yields high-resolution structural insights into β2-adrenergic receptor function. *Science*, 25 October 2007 (10.1126/science.1150609)

Cherezov, V., Peddi, A., Muthusubraniam, L., Zheng, Y.F., Caffrey, M. A robotic system for crystallizing membrane and soluble proteins in lipidic mesophases. *Acta Cryst* (2004) **D60**, 1795

Acknowledgments

The authors acknowledge the support of Janet Smith, Robert Fischetti and Nukri Sanishvili at the GM/CA-CAT beamline at the Advanced Photon Source, for assistance in development and use of the minibeam and beamtime. The GM/CA-CAT beamline (23-ID) is supported by the National Cancer Institute (Y1-CO-1020) and the National Institute of General Medical Sciences (Y1-GM-1104). This work was supported in part by the NIH Roadmap Initiative grant P50 GM073197.
The authors acknowledge Dan Rosenbaum and Brian Kobilka from Stanford University, Haiyan Chu and Phillip Low from Purdue University for providing protein samples used in this work, and Martin Caffrey and Yuan Zheng from The Ohio State University for the generous loan of the *in meso* robot.